

# Gas adsorption properties of mesoporous $\gamma$ -alumina prepared by a selective leaching method

Kiyoshi Okada,\* Takahiro Tomita and Atsuo Yasumori

Department of Inorganic Materials, Tokyo Institute of Technology, O-okayama, Meguro, Tokyo 152-8552, Japan. E-mail: kokada@o.cc.titech.ac.jp

Received 7th August 1998, Accepted 27th September 1998

Gas adsorption properties of mesoporous  $\gamma$ -Al<sub>2</sub>O<sub>3</sub> prepared by the selective leaching method were investigated using various adsorbate gases. The mesoporous  $\gamma$ -Al<sub>2</sub>O<sub>3</sub> was prepared by calcining kaolinite to form a microtexture of fine  $\gamma$ -Al<sub>2</sub>O<sub>3</sub> grains dispersed in a matrix of amorphous SiO<sub>2</sub> followed by selective leaching of amorphous SiO<sub>2</sub> from the microtexture. The mesopores were formed inside the pseudomorphic hexagonal platy particles of kaolinite. The specific surface area, total pore volume and pore size measured at 77 K using N<sub>2</sub> gas were ca. 240 m<sup>2</sup> g<sup>-1</sup>, 0.7 ml g<sup>-1</sup> and 6 nm, respectively. The gas adsorption isotherms of polar molecules such as water, methanol and butan-1-ol showed type IV isotherms (IUPAC classification) while those of non-polar molecules such as cyclohexane showed type V isotherms. The  $\gamma$ -Al<sub>2</sub>O<sub>3</sub> was therefore recognized as having hydrophilic surface characteristics. The onset of adsorption of these gases in the low relative pressure ( $P/P_0$ ) region was methanol > water > butan-1-ol > cyclohexane, this order corresponding to the affinity between the adsorbate gas and surface of the  $\gamma$ -Al<sub>2</sub>O<sub>3</sub> and also reflecting the steric effect of adsorbate gas. The fractal dimension obtained from the BET monolayer adsorption capacity plot was 2.1, indicating a smooth surface. The gas adsorption properties of the  $\gamma$ -Al<sub>2</sub>O<sub>3</sub> are discussed and compared with commercial  $\gamma$ -Al<sub>2</sub>O<sub>3</sub> and Al<sub>2</sub>O<sub>3</sub>-SiO<sub>2</sub> gel.

## Introduction

Since  $\gamma$ -Al<sub>2</sub>O<sub>3</sub> has a number of superior properties as a porous material, it has been widely used in industry as a catalyst, catalyst support and adsorbent. In order to improve the porous properties of  $\gamma$ -Al<sub>2</sub>O<sub>3</sub>, many preparation methods<sup>1-5</sup> have been reported which achieve enhancement of the properties by controlling the primary particle size. Various methods have also been used to control the microtexture of  $\gamma$ -Al<sub>2</sub>O<sub>3</sub> aggregates. We have reported a new preparation method of  $\gamma$ -Al<sub>2</sub>O<sub>3</sub> from the clay mineral kaolin [Al<sub>2</sub>(OH)<sub>4</sub>Si<sub>2</sub>O<sub>5</sub>] by a selective leaching method,<sup>6</sup> in which kaolin is calcined at ca. 1000 °C and converted into a mixture of  $\gamma$ -Al<sub>2</sub>O<sub>3</sub> and amorphous silica. Since the calcined kaolin retains pseudomorphic particles of the original kaolin with a microstructure consisting of a nanocomposite of very fine  $\gamma$ -Al<sub>2</sub>O<sub>3</sub> grains several nm in size uniformly dispersed in a matrix of amorphous SiO<sub>2</sub>, mesoporous  $\gamma$ -Al<sub>2</sub>O<sub>3</sub> can be prepared by selective leaching of the amorphous SiO<sub>2</sub> from the pseudomorph particles. As a result, the fine  $\gamma$ -Al<sub>2</sub>O<sub>3</sub> grains which remain in the microtexture are inter-connected by residual amorphous SiO<sub>2</sub> and form mesopores in the pseudomorph particles. Since the  $\gamma$ -Al<sub>2</sub>O<sub>3</sub> prepared by the selective leaching method has such a unique microtexture, it retains a high surface area at high temperatures, *i.e.*, it has high thermal stability<sup>7</sup> and shows unique and interesting water vapor adsorption properties.<sup>8</sup>

The present paper examines the gas adsorption properties of  $\gamma$ -Al<sub>2</sub>O<sub>3</sub> prepared by the selective leaching method using adsorbate gases with various molecular shapes and different polarities. The results are compared with commercial  $\gamma$ -Al<sub>2</sub>O<sub>3</sub> and Al<sub>2</sub>O<sub>3</sub>-SiO<sub>2</sub> gel to elucidate surface properties of the  $\gamma$ -Al<sub>2</sub>O<sub>3</sub>.

## Experimental

Kaolinite from Georgia, USA, was used as the starting material. As listed in Table 1, the chemical composition of this starting material is close to the ideal composition of kaolinite [2SiO<sub>2</sub>·Al<sub>2</sub>O<sub>3</sub>·2H<sub>2</sub>O], *i.e.* SiO<sub>2</sub>=46.51, Al<sub>2</sub>O<sub>3</sub>=39.54 and

H<sub>2</sub>O=13.95 mass%. A small amount of TiO<sub>2</sub> impurity was present as anatase and rutile in the sample. The starting material was calcined at 950 °C for 24 h using heating and cooling rates of 15 and 20 °C min<sup>-1</sup>, respectively. The calcined material (3 g) was dispersed in 250 ml of aqueous 4 M KOH at 90 °C and stirred for 1 h. After leaching, the sample was washed with 0.5 M KOH and then washed a further three times with deionized water to remove dissolved ions. The suspension was then centrifuged and the resulting powder dried at 110 °C overnight. For comparison, commercially available high purity  $\gamma$ -Al<sub>2</sub>O<sub>3</sub> (AKP-G015, Sumitomo Chemicals) and Al<sub>2</sub>O<sub>3</sub>-SiO<sub>2</sub> gel (Neobead DS-5, Mizusawa Chemicals) were used as reference materials.

The phases formed in the samples were studied by powder X-ray diffraction (XRD) using a Rigaku Geigerflex diffractometer with monochromated Cu-K $\alpha$  radiation. The chemical compositions were determined by X-ray fluorescence (XRF) using Rigaku RIX2000 and RIX3000 spectrometers. The microtexture of the samples was observed by field-emission scanning electron microscopy (FE-SEM) using a JEOL JCM-890S instrument. The specific surface area was measured by the BET method<sup>9</sup> using nitrogen gas as adsorbate at -196 °C with a Quanta Chrome Autosorb-1 instrument. The pore size distribution was calculated in the radius range from 1 to 100 nm by the BJH method<sup>10</sup> using the desorption isotherm. Gas adsorption-desorption isotherms were measured at 25 °C by automatic gas adsorption apparatus using a Japan Bel Belsorp 18. The adsorbates used were deionized water, a special grade of methanol (Shuzui Kitaro Co.), butan-1-ol (Wako Pure Chemicals) and cyclohexane (Wako Pure Chemicals). They were pre-treated using zeolite 3A (Wako Pure Chemicals) to remove any contaminating water. The alumina samples were evacuated at 300 °C for >4 h until the pressure in the vessel dropped below 5  $\times$  10<sup>-3</sup> Torr. The duration of each measurement point was set at 1000 s. The measured relative pressure ( $P/P_0$ ) range was 0-0.9 in the adsorption and 0.9-0.1 in the desorption experiments except for the methanol runs, in which the measurements were made only to  $P/P_0$ =0.7 because of limitations of the apparatus.

**Table 1** Chemical composition and porous properties of samples

Sample	Chemical composition (mass%)					Surface area/m <sup>2</sup> g <sup>-1</sup>	Pore volume/ml g <sup>-1</sup>
	Al <sub>2</sub> O <sub>3</sub>	SiO <sub>2</sub>	TiO <sub>2</sub>	K <sub>2</sub> O	Fe <sub>2</sub> O <sub>3</sub>		
Original kaolinite	38.3	45.2	1.44	0.11	0.76	9.9	0.09
Selectively leached $\gamma$ -Al <sub>2</sub> O <sub>3</sub>	84.0	6.8	5.5	1.4	1.0	244	0.72
$\gamma$ -Al <sub>2</sub> O <sub>3</sub> (AKP-G015)	100	0	0	0	0	139	1.22
Al <sub>2</sub> O <sub>3</sub> -SiO <sub>2</sub> gel (DS-5)	70.5	24.5	0	0	0	313	0.51

## Results and discussion

### Characterization of the samples

As reported in previous papers,<sup>5-7</sup> the calcined and KOH leached sample has mesopores of uniform pore size of *ca.* 3 nm radius. The porous properties and chemical composition of the sample prepared in the present study are listed in Table 1 and are in good agreement with those reported elsewhere.<sup>5-7</sup> Fig. 1 shows the pore size of this sample lies in a narrow distribution around 3 nm radius. The data for the reference materials of commercially available  $\gamma$ -Al<sub>2</sub>O<sub>3</sub> and Al<sub>2</sub>O<sub>3</sub>-SiO<sub>2</sub> gel are also given in Table 1 and Fig. 1, and show different pore sizes from the present  $\gamma$ -Al<sub>2</sub>O<sub>3</sub>. The pore size of the reference  $\gamma$ -Al<sub>2</sub>O<sub>3</sub> (AKP-G015) is larger than those of the other two samples and the pore size distribution is relatively broad. The pore size of the Al<sub>2</sub>O<sub>3</sub>-SiO<sub>2</sub> gel (DS-5) is smaller than those of the other samples, but with a rather broad bimodal size distribution consisting of a relatively sharp peak at *ca.* 1.9 nm radius and very broad peak at *ca.* 3-4 nm. The order of specific surface areas of these samples was AKP-G015 < present  $\gamma$ -Al<sub>2</sub>O<sub>3</sub> < DS-5, this order being correlated with the pore size. On the other hand, the total pore volumes of these samples showed the opposite trend with specific surface area.

The XRD pattern of the calcined sample showed broad peaks assigned to  $\gamma$ -Al<sub>2</sub>O<sub>3</sub> and a halo arising from amorphous SiO<sub>2</sub> which disappeared after leaching. Corresponding to this XRD pattern change, the chemical composition revealed a reduction of SiO<sub>2</sub> upon leaching (Table 1). The microtextures of the original and leached samples were observed by FE-SEM (Fig. 2). Photographs show that the sample preserves the hexagonal platy particle shape of the original kaolinite even after calcination and leaching, but with apparent changes in the surface of pseudomorphic particles. Very fine grains of  $\gamma$ -Al<sub>2</sub>O<sub>3</sub> were observed on the surface of the particles, shown

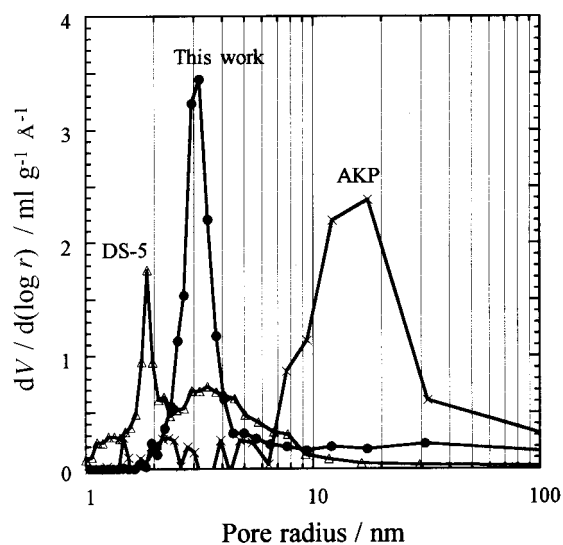


**Fig. 1** Pore size distributions of the present  $\gamma$ -Al<sub>2</sub>O<sub>3</sub> prepared by selective leaching, commercial  $\gamma$ -Al<sub>2</sub>O<sub>3</sub> (AKP-G015) and Al<sub>2</sub>O<sub>3</sub>-SiO<sub>2</sub> gel (DS-5).

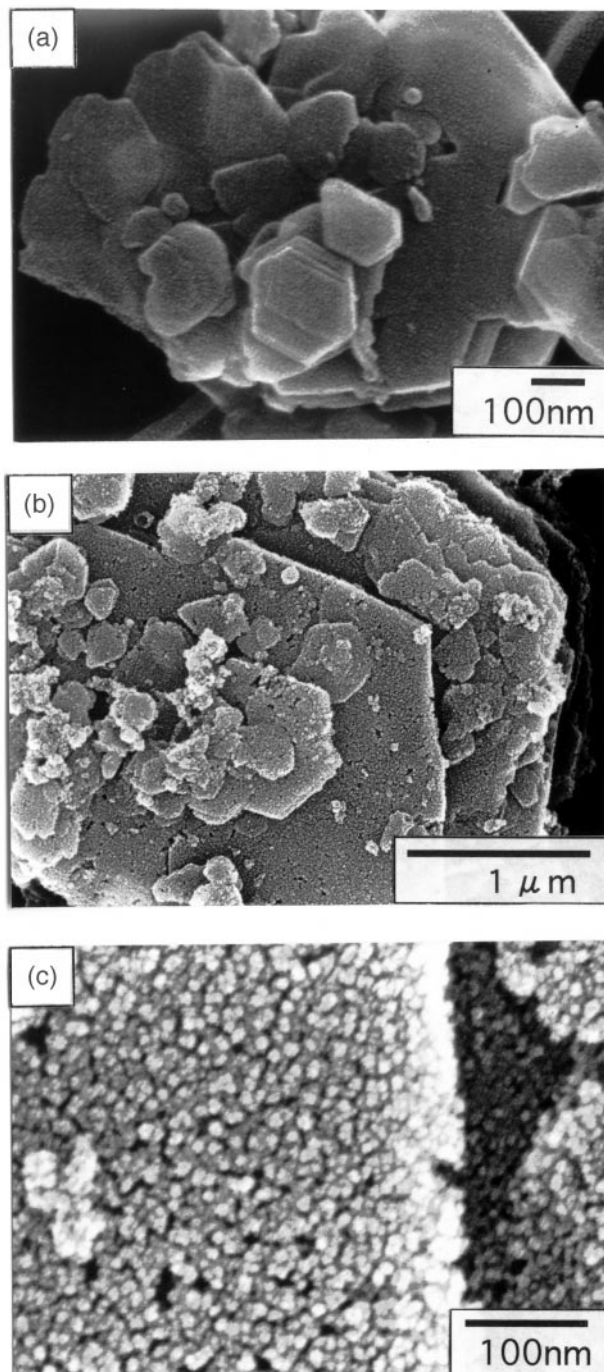


**Fig. 2** FE-SEM photographs of the selectively leached  $\gamma$ -Al<sub>2</sub>O<sub>3</sub>: (a) original sample, (b) leached sample and (c) leached sample with high magnification.

in Fig. 2(b) and (c) to be several nm in size. The spaces between the fine  $\gamma$ -Al<sub>2</sub>O<sub>3</sub> grains formed by selective leaching of amorphous SiO<sub>2</sub> from the matrix correspond to the mesopores in this sample. The fine  $\gamma$ -Al<sub>2</sub>O<sub>3</sub> grains are of uniform size and are distributed uniformly in the pseudomorphic

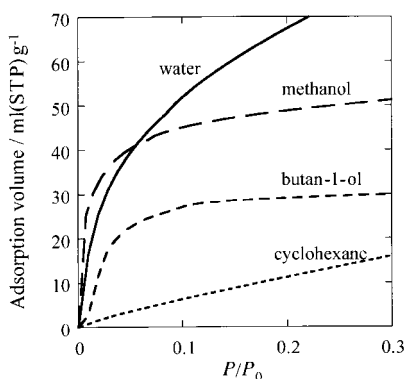


**Fig. 3** Adsorption isotherms of various adsorbates on the selectively leached  $\gamma\text{-Al}_2\text{O}_3$ .

particles, yielding uniformly sized mesopores with a narrow pore size distribution. The  $^{29}\text{Si}$  MAS NMR spectra of this sample showed the  $\text{Q}^4$  structure unit of  $\text{SiO}_4$  tetrahedra, as well as a framework structure and a  $\text{Q}^0$  structure unit representing  $\text{SiO}_4$  tetrahedra incorporated in the  $\gamma\text{-Al}_2\text{O}_3$ .<sup>11</sup> Since amorphous  $\text{SiO}_2$ , which has the  $\text{Q}^4$  structure, is present as the matrix of the microtexture of the calcined sample and the pseudomorphic particle shape is retained after the leaching treatment, these fine  $\gamma\text{-Al}_2\text{O}_3$  grains are thought to be connected by residual amorphous  $\text{SiO}_2$ .

#### Gas adsorption properties of the samples

Fig. 3 shows gas adsorption isotherms ( $0 < P/P_0 \leq 0.3$ ) of the present  $\gamma\text{-Al}_2\text{O}_3$  for the polar adsorbates water, methanol, butan-1-ol and the non-polar molecule cyclohexane. The adsorption isotherms of polar and non-polar molecules are different; all the polar molecules show convex isotherms indicating the strong affinity of these molecules for the surface of the  $\gamma\text{-Al}_2\text{O}_3$ , *i.e.* hydrophilic behavior. On the other hand, the adsorption of cyclohexane shows an almost linear relationship with  $P/P_0$ , thus, its affinity for  $\gamma\text{-Al}_2\text{O}_3$  is weak. Differences can also be seen in the isotherms of the three polar molecules. The isotherms of the two alcohols showed a steep increase of adsorption in the low  $P/P_0$  range, reaching a plateau in the medium  $P/P_0$  range, however the  $P/P_0$  value at which this increase commenced was much lower for methanol than for butan-1-ol. By contrast, the water vapor adsorption isotherm was a different shape to those of the alcohols, increasing continuously with increasing  $P/P_0$  up to the medium  $P/P_0$  range and without a plateau. The difference in the adsorption of these four different molecules is shown schematically in Fig. 4. The hydrophilic surface of the present  $\gamma\text{-Al}_2\text{O}_3$  contains OH groups which absorb water vapor by forming hydrogen

bonds with surface OH groups of the  $\gamma\text{-Al}_2\text{O}_3$ . As depicted schematically in Fig. 4, the first layer of adsorbed water vapor is also able to form hydrogen bonds with further water vapor molecules to form second and third adsorbed layers, successively leading to multi-layer adsorption with increasing  $P/P_0$ . On the other hand, alcohol molecules adsorb on the surface of the  $\gamma\text{-Al}_2\text{O}_3$  by forming hydrogen bonds between their OH groups and the surface OH groups of the  $\gamma\text{-Al}_2\text{O}_3$ . In the case of methanol, this adsorption occurs steeply and starts from very low  $P/P_0$  because the affinity of methanol for  $\gamma\text{-Al}_2\text{O}_3$  is strong and the steric hindrance of the methanol molecule is small. The isotherm of methanol starts at lower  $P/P_0$  than that of water vapor, suggesting that the adsorption energy of methanol is higher than that of water vapor. On the other hand, the isotherm of butan-1-ol shows an induction region of adsorption at very low  $P/P_0$  but with increasing  $P/P_0$  it increases steeply, behaving similarly to methanol above a certain  $P/P_0$ . This induction region is considered to reflect the steric hindrance of butan-1-ol, which has a molecular length (0.8–0.9 nm) estimated to be about twice that of methanol. The adsorption of the first layer of alcohol molecules occurs in such a way that the  $\text{CH}_3$  groups face away from the surface as depicted in Fig. 4. This changes the surface property from hydrophilic to hydrophobic after adsorption of the first layer, explaining the plateau in the alcohol isotherm. Since the steric hindrance of butan-1-ol is larger than that of methanol, the plateau in the isotherm of butan-1-ol is flatter than for methanol. In contrast to the hydrogen bond adsorption mechanism in water vapor and alcohols, the adsorption of cyclohexane is considered to occur by physical adsorption, explaining the linear correlation with  $P/P_0$ .

Generally, the surface roughness of porous materials is evaluated in terms of its fractal dimension. Pfeifer and Avnir<sup>12</sup> give the following formula to calculate the fractal dimension of porous materials from adsorption data for different molecular size adsorbates

$$\log(v_m) = -(D/2) \log(a_m) + C$$

where,  $v_m$ ,  $D$ ,  $a_m$  are the BET monolayer adsorption capacity, surface fractal dimension and cross-sectional area of the adsorbed molecules, and  $C$  is a constant. Fig. 5 shows a plot of  $\log(v_m)$  vs.  $\log(a_m)$  for the present  $\gamma\text{-Al}_2\text{O}_3$  prepared by the selective leaching method and for commercial  $\gamma\text{-Al}_2\text{O}_3$  (AKP-G015). Both data sets show a good linear correlation, from which the fractal dimensions were calculated from the slopes as 2.1 and 2.2 for the present  $\gamma\text{-Al}_2\text{O}_3$  and commercial  $\gamma\text{-Al}_2\text{O}_3$ , respectively. Since rough and smooth surface states correspond to fractal dimensions of 3 and 2, respectively, the present  $\gamma\text{-Al}_2\text{O}_3$  has a rather smooth surface.

Fig. 6 shows a comparison of the adsorption–desorption isotherms of various adsorbates on the present  $\gamma\text{-Al}_2\text{O}_3$  and

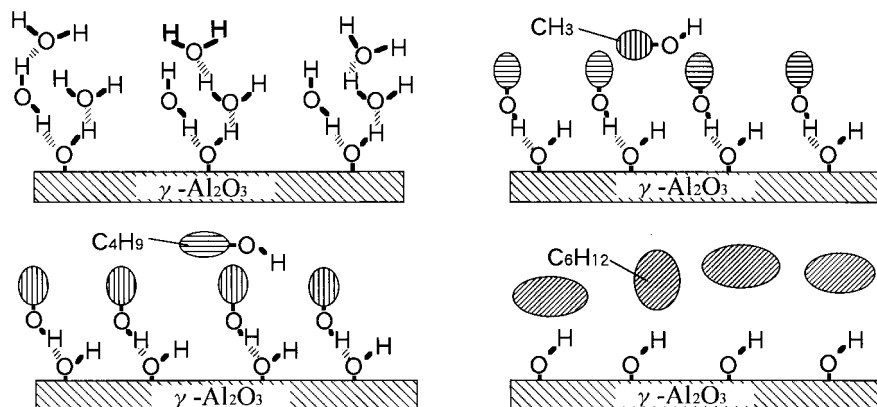


**Fig. 4** Schematic illustrations of adsorption mechanisms for various adsorbates.

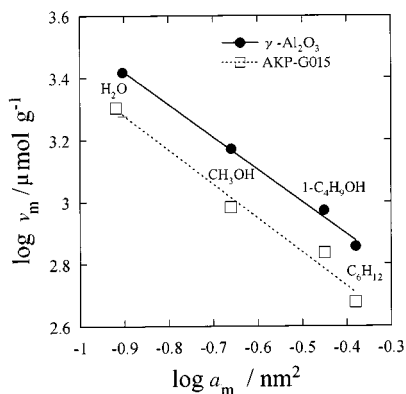


**Fig. 5** BET monolayer adsorption capacity ( $v_m$ ) of various adsorbates on the present  $\gamma$ - $\text{Al}_2\text{O}_3$  and  $\gamma$ - $\text{Al}_2\text{O}_3$  (AKP-G015) as a function of cross section ( $a_m$ ) of adsorbate.

the reference samples. Similar trends are observed in the isotherms of all the adsorbates on corresponding samples. Adsorption at low  $P/P_0$  increases in the order  $\gamma$ - $\text{Al}_2\text{O}_3$  (AKP-G015) < the present  $\gamma$ - $\text{Al}_2\text{O}_3$  <  $\text{Al}_2\text{O}_3$ - $\text{SiO}_2$  gel (DS-5). This tendency is suggested to correlate with the specific surface area, pore size and also the hydrophilicity of the samples. We discussed the hydrophilicity of these samples in a previous paper<sup>8</sup> and concluded that the hydrophilicity shows a tendency to decrease with increase of  $\text{SiO}_2$  content in the samples. On the other hand, the maximum adsorption of these samples increases in the order  $\gamma$ - $\text{Al}_2\text{O}_3$  (AKP-G015) <  $\text{Al}_2\text{O}_3$ - $\text{SiO}_2$  gel (DS-5) < the present  $\gamma$ - $\text{Al}_2\text{O}_3$ . This should correspond to the sample pore volume giving rise to capillary condensation up to  $P/P_0=0.9$ . Since the changes in the adsorption isotherms

in the high  $P/P_0$  range correspond to the capillary condensation, the slope ratio is related to the pore size distribution. We therefore conclude that the steep change in the isotherms of the present  $\gamma$ - $\text{Al}_2\text{O}_3$  is due to its narrow pore size distribution. The present  $\gamma$ - $\text{Al}_2\text{O}_3$  contains a small amount of  $\text{K}_2\text{O}$  contamination from the leaching treatment. This impurity may have some influence on the adsorption property. Previously it was found to show only little influence in lowering the starting value of  $P/P_0$  for the capillary condensation.<sup>8</sup>

## Conclusions

The gas adsorption properties of  $\gamma$ - $\text{Al}_2\text{O}_3$  prepared by a selective leaching method were investigated using four adsorbates with different molecular sizes and polarities (water, methanol, butan-1-ol and cyclohexane). The following results were obtained.

- (1) Since the leached  $\gamma$ - $\text{Al}_2\text{O}_3$  showed a strong affinity for polar molecules but a weak affinity for non-polar molecules, the surface appears to have a hydrophilic character.
- (2) The convex shape of the isotherms differed for the different adsorbates in a manner which could be related to the adsorption mechanism.
- (3) The fractal dimension of the present  $\gamma$ - $\text{Al}_2\text{O}_3$  was calculated to be 2.1, corresponding to a rather smooth surface.
- (4) The present  $\gamma$ - $\text{Al}_2\text{O}_3$  showed a very steep increase and decrease of the isotherms in the high  $P/P_0$  range due to capillary condensation, consistent with a narrow pore size distribution in this sample.

## Acknowledgments

We are grateful to Dr Katsunori Kosuge of National Institute for Resources and Environment for fruitful suggestions on

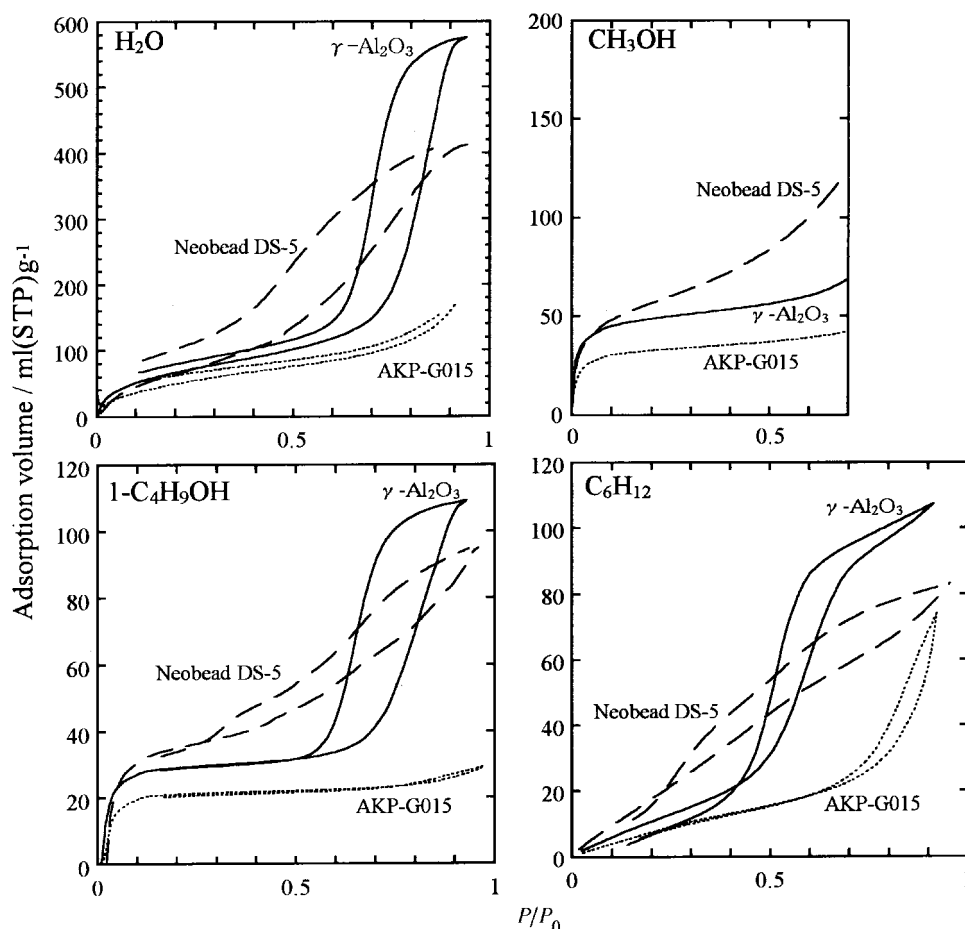


**Fig. 6** Adsorption-desorption isotherms of various adsorbates in the present  $\gamma$ - $\text{Al}_2\text{O}_3$ ,  $\gamma$ - $\text{Al}_2\text{O}_3$  (AKP-G015) and  $\text{Al}_2\text{O}_3$ - $\text{SiO}_2$  gel (DS-5).

adsorption experiments and also grateful to Dr K.J.D. MacKenzie of New Zealand Institute for Industrial Research and Development for proof reading and editing of this paper. A part of this work was supported by a Grant-in-Aid for Scientific Research (B) (No.09450240) by the Ministry of Education, Science, Culture and Sports, Japan and also by TOSTEM Foundation.

## References

- 1 N. G. Papayannakos, A. M. Thomas and V. E. Kaloidas, *Microporous Mater.*, 1993, **1**, 413.
- 2 T. Ono, Y. Oguchi and O. Togari, in *Preparation of Catalysis III*, ed. G. Poncelet, P. Grange and P. A. Jacobs, Elsevier, Amsterdam, 1983, p. 631.
- 3 Y. Mizushima and M. Hori, in *EUROGEL'91*, ed. S. Vilminot, R. Nass and H. Schmidt, Elsevier, Amsterdam, 1992, p. 195.
- 4 D. L. Trimm and A. Stainislaus, *Appl. Catal.*, 1986, **21**, 215.
- 5 R. F. Vogel, G. Marcelin and W. L. Kehl, *Appl. Catal.*, 1984, **12**, 237.
- 6 K. Okada, H. Kawashima, Y. Saito, S. Hayashi and A. Yasumori, *J. Mater. Chem.*, 1995, **5**, 1241.
- 7 Y. Saito, T. Motohashi, S. Hayashi, A. Yasumori and K. Okada, *J. Mater. Chem.*, 1997, **7**, 1615.
- 8 K. Okada, Y. Saito, M. Hiroki, T. Tomita and S. Tomura, *J. Porous Mater.*, 1997, **4**, 253.
- 9 S. Brunauer, P. H. Emmett and E. Teller, *J. Am. Chem. Soc.*, 1938, **60**, 309.
- 10 E. P. Barrett, L. G. Joyner and P. P. Halenda, *J. Am. Chem. Soc.*, 1951, **73**, 373.
- 11 K. J. D. MacKenzie, J. S. Hartman and K. Okada, *J. Am. Ceram. Soc.*, 1996, **79**, 2980.
- 12 P. Pfeifer and D. Avnir, *J. Chem. Phys.*, 1983, **79**, 3558.

Paper 8/06240D